

Using the CO₂DGM model to characterize and to diagnose electric thrusters meant for propulsion near Mars or Venus

Konstantinos Katsonis[†] and Chloe Berenguer**

** DEDALOS Ltd*

Vassilissis Olgas 128, 54645 Thessaloniki, Greece

katsonis.dedalos@gmail.com – berenguer.dedalos@gmail.com

[†] Corresponding Author

Abstract

The CO₂DGM detailed global model is used to characterize electric thrusters breathing CO₂. The latter are of interest to Mars and Venus artificial satellites and spacecraft propulsion in their vicinity. CO₂DGM results are illustrated by diagrams giving the composition of the plasma components and ionization percentages containing isothermal, isobaric and isoenergetic curves which describe the thruster functioning for various regimes.

The model incorporates data concerning detailed structure and reactions involving oxygen and carbon species and molecules composed from them, including their ions. Thus, spectral lines intensity of the main thruster constituents is obtained, allowing for optical emission spectroscopy diagnostics.

1. Introduction

Using of CO₂ as Electric Thruster (ET) propellant is of interest to propulsion of satellites and spacecrafts in the vicinity of stellar bodies possessing atmospheres composed mainly of this molecule. Thus, CO₂ fueled ETs are considered for propulsion near Mars and Venus following *In Situ* Resources Utilization (ISRU) technology for satellites and spacecrafts [1]. CO₂DGM, a Detailed Global Model (DGM) developed by DEDALOS Ltd specifically for CO₂ fed ETs of various types, can be used for theoretical characterization and non-perturbing Optical Emission Spectroscopy (OES) diagnostics of prototypes developed for on ground experiments [2,3] increasing the TRL number prior to the IOD and IOV steps. Once TRL 9 is obtained, the ISRU type thruster applications in industry will become possible for Solar system exploration in general [3], up to missions to its more distant planet Neptune [4]. In so doing, atmospheres containing other than CO₂ constituents, notably nitrogen and oxygen [5,6] and hydrogen and helium [7,8] have been addressed.

As usually, results obtained by CO₂DGM are often presented under the following forms:

- Plasma Components Composition (PCC) diagrams, giving the composition of the plasma components as a function of the pressure (p) or of the absorbed power (P_{abs})
- Functioning Diagrams (FD) which contain crossing isothermal and isoenergetic curves and provide ionization percentage also as a function of p or P_{abs}
- Theoretical first and second oxygen and carbon spectra belonging to given conditions, which allow for OES diagnostics.

On the basis of CO₂DGM results, preview of the main species densities in a prototype, namely CO₂, CO, oxygen and carbon, including their ions and molecules, together with the electron density n_e and temperature T_e values is obtained. Besides p or P_{abs} , the elaborated PCC diagrams incorporate the ET form factors and also values of CO₂ propellant feed, through the total Flow Rate (Q_{TOT}). Analysis of the corresponding functioning regimes is obtained and illustrated using FDs.

Obtained theoretical spectra of O I, O II and C I, C II, necessary for OES diagnostics, are here presented and commented. In order to thoroughly support OES diagnostics, extended sets of data concerning the neutral and the singly, doubly and trebly ionized oxygen species have been specifically included in the DGM basic equations [1]. The latter consist of a “power balance” equation plus the well-known “statistical equations” set addressing the main plasma species. Thus, CO₂DGM becomes able to describe the effects of the present atomic and ionic structures in a realistic manner, leading also to detailed calculation of the theoretical spectral lines belonging to the ET plasma. In addition, data pertaining to the molecules of interest are also included in the model.

CO₂DGM evaluates the P_{ABS} losses belonging to the thruster functioning conditions. Thus, it results to realistic mean values of the thruster plasma parameters, as was reported elsewhere [9,10].

Characterization and OES diagnostics of prototype thrusters fed by CO₂ are presented and discussed using CO2DGM results. Although molecular CO₂ spectra are also very present in the plasma, especially for low P_{ABS} values, only OES diagnostics based in the visible and UV part of the atomic and ionic oxygen and carbon species spectral emission is addressed, with oxygen and carbon containing species which are present in considerable amount. The choice of the atoms or ions of which the spectra are to be taken as a basis of the OES diagnostics is made according to their relative abundance in the plasma. Spectral acquisition may contribute also to the model validation, by comparison of results obtained using experimental spectra of neutral, singly and doubly ionized species with the theoretical ones. Spectral acquisition can be further lead to the surfaces erosion level.

In all, CO2DGM results are used in controlling, diagnosing and optimizing the functioning of the thruster. We focus here on low pressure CO₂ plasma properties, which is of interest to ISRU type electric thrusters fed by the Mars Atmosphere (MAtm). In view of previous studies results [11], influence of the nitrogen presence in the MAtm on the functioning of ETs breathing this atmosphere is neglected. Spectroscopic measurements can also evaluate the presence of various components coming from erosion, which according to the ET type and to the amount of the oxygen presence could become considerable.

CO2DGM is also of interest to the initial phase of entry in the atmospheres of Mars [12]. Note that, in this case the pressure varies very fast and special attention must be payed to its variation. Applicability study of the model for application in various conditions is given in [13].

A wide range of P_{ABS} values is addressed, going from 0.5 kW to 4 kW. Evidently, the P_{ABS} of interest depends on the feed technology selected (direct CO₂ breathing or propellant collection in an adequate vessel), on the thruster type and form factor and on the amount of the used propellant which is strongly related to the available absorbed power. While PCC diagrams illustrate the constitution of the propellant inside the ET as calculated by the model for given conditions, a synoptic FD, based on more than one PCC, contribute to analyze the thruster functioning. FDs give the ionization percentage as a function of the pressure by two sets of crossing curves, with each of them pertaining to a given value of P_{ABS} or of T_e. An alternate form of FD diagrams is also possible, describing the thruster functioning dependence on P_{ABS}, with the parametric curves referring to values of p and T_e.

Description of CO2DGM model is not given here. The model fundamentals, allowing for the important ISRU support of ETs provided by this type of modeling and by the concomitant OES diagnostics, have been described elsewhere [1].

In Section 2 of this contribution, the composition and the properties of plasma created from CO₂ in various conditions which are primarily of interest to propulsion in the Mars and Venus vicinities are investigated. This concerns medium and high power class CO₂-fuelled ET prototypes with Q_{TOT} of 40 sccm. Sufficient P_{ABS} should be available in order to sustain ionization convenient for the sought thrust. A FD which is obtained on the basis of CO2DGM results for various functioning conditions is addressed in Section 3. In Section 4, typical theoretical CO₂ spectra corresponding to a case addressed in previous sections are compared with experimental ones, leading to illustration of OES diagnostics results. Finally, conclusions of this work are contained in Section 5.

2. PCCs and concomitant diagrams obtained for CO₂ –fuelled ETs

Results obtained by CO2DGM, pertaining to the presence of various components of the CO₂ -fed ETs plasma functioning under various conditions, are analyzed in the following on the basis of PCC diagrams. Percentages of CO₂ and CO₂⁺ and of other neutral and ionized species created in the thruster plasma, together with the total ionization percentage ξ_{TOT} and the electron temperatures T_e which are evaluated by the model, are also occasionally presented in concomitant diagrams. The latter provide a complete overview of the corresponding plasma state.

A typical ET form factor of $R = 2$ cm and $L = 18$ cm resulting to a plasma volume larger than previously [14] is chosen here, with Helicon type thrusters applied in MAtm and Venus Atmosphere (VAtm) propulsion and in Mars and Venus missions in mind. Also, sufficient fuel availability is presumed, due to the ISRU technology addressed. The considered CO₂ feed of 40 sccm is expected to lead to a sufficiently ionized propellant, provided enough power is made available in order to reach convenient absorbed power P_{ABS} values. In our examples, the P_{ABS} values are varying from 0.5 kW up to 4 kW, but only the two cases of 1 kW and 4 kW are addressed specifically in this section. Fundamental results as total density n_{TOT}, electron density n_e and the densities of the main plasma constituents obtained by CO2DGM are presented in the corresponding PCC diagrams, which are spanning a pressure region going from 1 mTorr to 10 mTorr.

For the considered form factor of $R = 2$ cm and $L = 18$ cm and a Q_{TOT} = 40 sccm, the plasma composition obtained by CO2DGM when the absorbed power is P_{ABS} = 1 kW is illustrated in the pressure depending log – log PCC diagram shown in Fig. 1. The total density n_{TOT} (magenta dashed curve) increases regularly with pressure, followed with a factor of around 0.5 by the electron density n_e (magenta dash dotted curve). CO₂⁺ density values (thick black curve with hollow triangles) which is the more abundant species follow with quite lower values, beginning at about 5.0x10¹¹ cm⁻³ and increasing for higher pressures. The ground level ($v = 0$) of carbon dioxide density values CO₂ (thin black points curve) begin with the same value for $p = 1$ mTorr with similar values, but increase rather slowly

with p . The electron density remains quite higher than this of CO_2^+ for all pressures, indicating considerable creation of ionized components other than CO_2^+ as are O^+ and CO^+ .

Neutral species as atomic oxygen (Tot O, red curve with hollow circles) and CO (blue curve with full triangles) and the quite less present C (green curve with full diamonds) are created but, except from the case of oxygen near 1 mTorr, the corresponding ions are more present. Presences of O and CO increase fast with pressure, while C presence starts from lower values and increases slowly. Presences of the corresponding ionized species O^+ (red curve with crosses), CO^+ (blue curve with crosses) and C^+ (green curve with empty diamonds) are considerable, with their densities increasing fast with pressure.

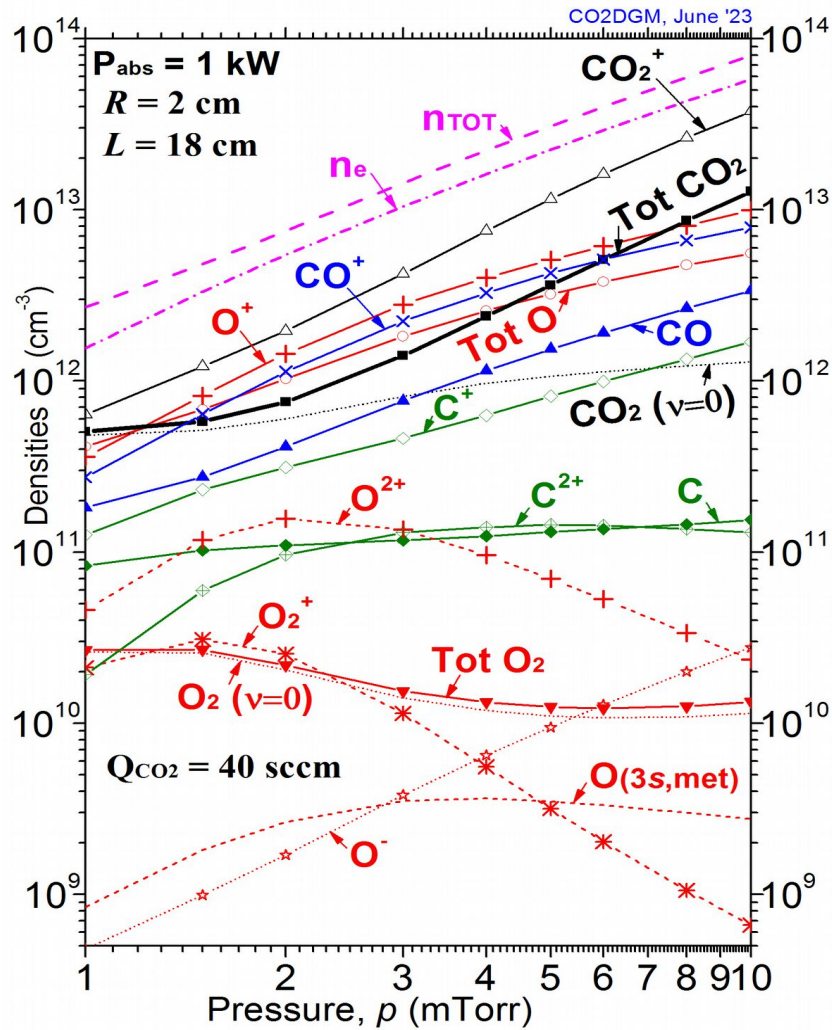


Figure 1. Pressure-dependent PCC for ET fueled by 40 sccm of CO_2 , for $P_{\text{abs}} = 1 \text{ kW}$

The lower part of Fig. 1. pertains to less abundant species. Among them are the twice ionized O^{2+} (red dashed curve with crosses) and C^{2+} (green curve with crossed diamonds) species. Both follow curves which have maxima slightly exceeding 10^{11} cm^{-3} , for pressures around 2 mTorr and 7 mTorr correspondingly. Abundance of O_2^+ (red dashed curve with crosses), although is similar with this of C^{2+} around 1 mTorr pressure, diminishes fast and falls to about one order of magnitude lower values for 10 mTorr. Inversely, the total abundance of the neutral oxygen molecules Tot O_2 (red curve with inverted full triangles) diminishes slowly to almost three times lower values when the pressure increases from 1 mTorr to 10 mTorr. The density of its vibrational state $v=0$ part (red dotted curve) is the bulk of the molecule presence for lower pressure values, while for higher ones its curve dissociates lightly from the Tot O_2 one, showing an appearance of vibrationally excited states.

At 1 mTorr pressure, density values of less than 10^9 cm^{-3} pertain to electronegativity (O^- , red dotted curve with stars) and to metastable O (3s, met) species (red short dashed curve). With increasing pressure, electronegativity increases steadily to values of about two orders of magnitude higher and the metastable oxygen reaches a density level of about $3 \times 10^9 \text{ cm}^{-3}$.

An alternative insight on the ET plasma ionization and electron temperature and also on the main components percentages as part of the total density n_{TOT} under the chosen conditions, is provided by Fig. 2, showing a diagram concomitant to the PCC of the Fig. 1. Symbols in this diagram are mostly self-explanatory with colours following mostly these of Fig. 1.

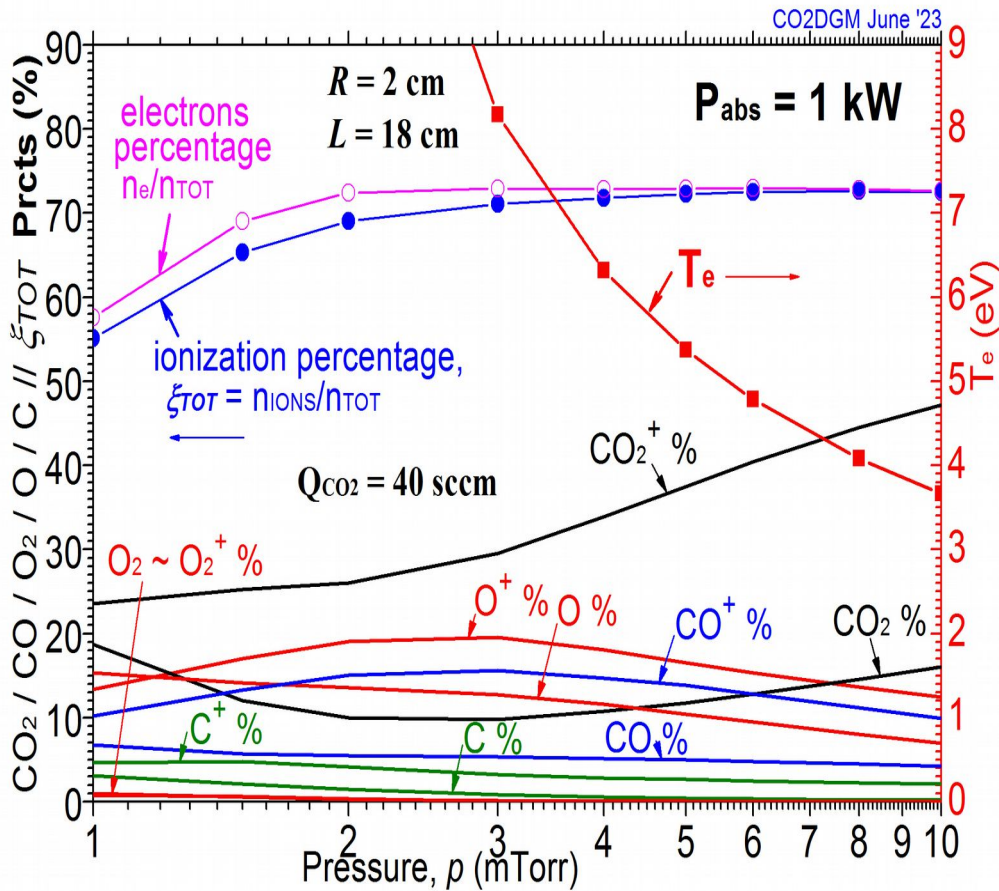


Figure 2. Pressure-dependent diagram, concomitant to the PCC of Fig. 1

Fig. 2 illustrates the percentages of the main plasma constituents and also the total ionization percentage $\xi_{TOT} = n_{IONS} / n_{TOT}$ (values given in the left side of the figure). The electron temperature T_e values are given in the right side of the figure. Note that for high pressures the ξ_{TOT} values are practically coinciding with these of the electron percentage n_e / n_{TOT} . The increasing difference among them pertaining to the lower pressures region shows a noticeable presence of doubly ionized species in this case. The observed concomitant fast increase of the T_e values (values given in the right side of the figure) when pressure diminish in the same region is considerable.

The neutral CO_2 percentage has a minimum at about 2.5 mTorr, while each of the O^+ and CO^+ percentages reach its maximum at slightly higher pressure values. The CO_2^+ percentage shows a slight difference from the CO_2 one for 1 mTorr, but for higher pressure values this difference becomes considerable, with the CO_2^+ percentage increasing continuously, exceeding finally 45 % for 10 mTorr. CO^+ percentage is always lower than the O^+ one, especially in the low pressure region. Percentages of the three most present formed neutrals, namely oxygen, carbon monoxide and carbon are lower than the corresponding singly ionized and diminish slowly when pressure increases, while the corresponding densities are increasing, according to the PCC of Fig. 1. Percentages of C^+ species have low values, diminishing with increasing pressure. Percentages of O_2 and O_2^+ species have comparable diminishing values, which are already very low even near 1 mTorr.

In case of a quite higher absorbed power of $P_{abs} = 4$ kW, a sustained ionization can be obtained. For the same form factor of $R = 2$ cm and $L = 18$ cm and Q_{TOT} of 40 sccm addressed in Figs. 1,2, the plasma composition obtained by CO2DGM when the absorbed power is $P_{ABS} = 4$ kW is illustrated in the pressure depending log – log PCC diagram of Fig. 3, which uses the same symbols with Fig. 1. The total density n_{TOT} increases regularly with pressure, following practically the electron density n_e . CO_2^+ density values have quite lower values (10^{13} cm^{-3}) than O^+ and CO^+ for $p = 10$ mTorr. The total carbon dioxide density values $Tot \text{ CO}_2$ have much lower values than in Fig. 1 due to the ample ionization. It is to be observed that the electron density remains much higher than this of O^+ which becomes now the

most abundant species, practically for all pressures except around 1 mTorr. This indicates abundant creation of ionized components other than O^+ (CO_2^+ , CO^+) and ionization promotion notably for p values in the 2 mTorr to 5 mTorr region.

Due to relatively low vibrational excitation presence in low pressures, the presence of CO_2 ($v=0$) species which coincides with this of CO_2 for low p values, increases very slowly with pressure while **total** CO_2 increases, approaching $2 \times 10^{12} \text{ cm}^{-3}$ for $p = 10 \text{ mTorr}$ pressure.

Neutral species as oxygen (**Tot O**) and **CO** and the quite less present **C** are created, but the corresponding ions are more present than in Fig. 1. Presences of **Tot O** and **CO** increase fast with pressure, while **C** presence remain around 10^{11} cm^{-3} density. Presences of the corresponding ionized species O^+ , CO^+ and C^+ are considerable, with their densities increasing fast with pressure.

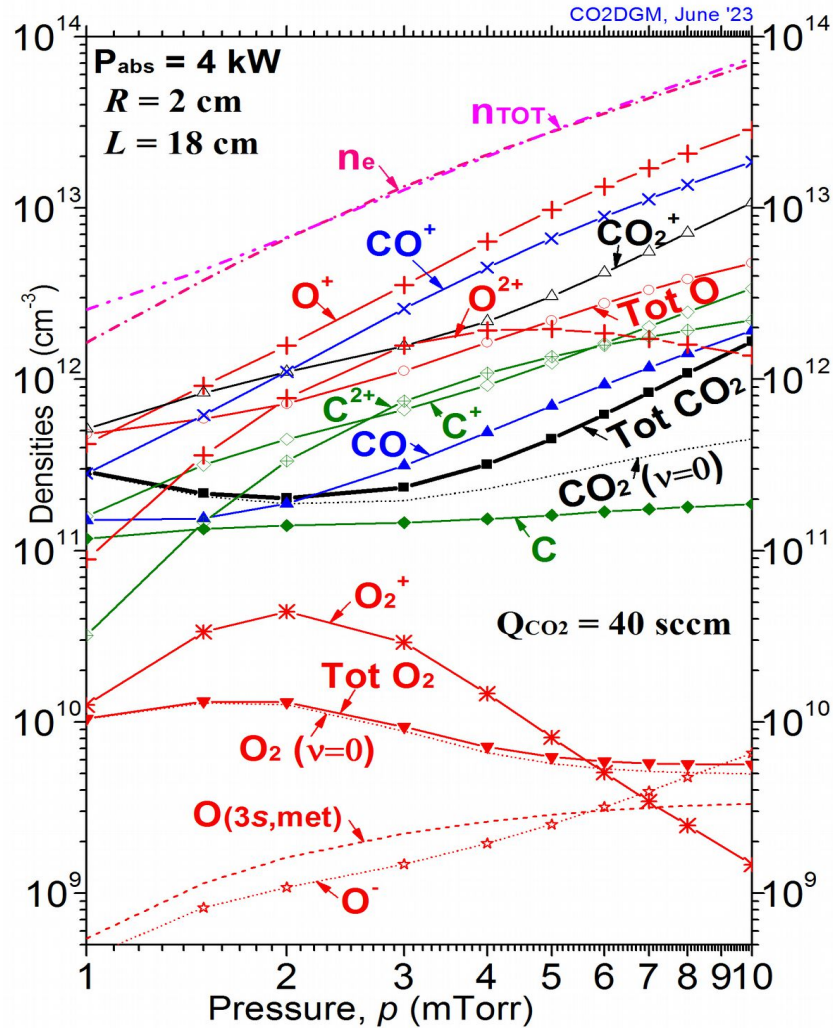


Figure 3. Pressure-dependent PCC for ET fueled by 40 sccm of CO_2 , for $P_{abs} = 4 \text{ kW}$

The twice ionized species are promoted in the upper part of Fig. 3 near the simply ionized ones, while the lower part of Fig. 3 pertains to less abundant species. Interestingly, the twice ionized O^{2+} and C^{2+} have considerable abundances, due to the high values of P_{abs} . Abundance of O_2^+ increases from 10^{10} cm^{-3} for low pressure values but strongly diminishes for higher pressure. Inversely, the total abundance of the neutral oxygen molecules **Tot O₂** diminishes slowly to two times lower values when the pressure increases from 1 mTorr to 10 mTorr. The density of its vibrational state $v=0$ part is the bulk of the molecule presence for lower pressure values, while for higher ones its curve dissociates lightly from the **Tot O₂** one, as in the case of $P_{abs} = 1 \text{ kW}$, showing an appearance of vibrationally excited states.

At 1 mTorr pressure, density values of less than 10^9 cm^{-3} pertain to electronegativity O^- and to metastable $O(3s, \text{met})$ species, but with increasing pressure, both increase slowly.

An extended insight on the ET plasma ionization and electron temperature and also on the main components percentages as part of the total density n_{TOT} under the chosen conditions is provided by Fig. 4, also for $P_{abs} = 4$ kW. The diagram shown in this figure is concomitant to the PCC of the Fig. 3, with symbols in this diagram mostly self-explanatory.

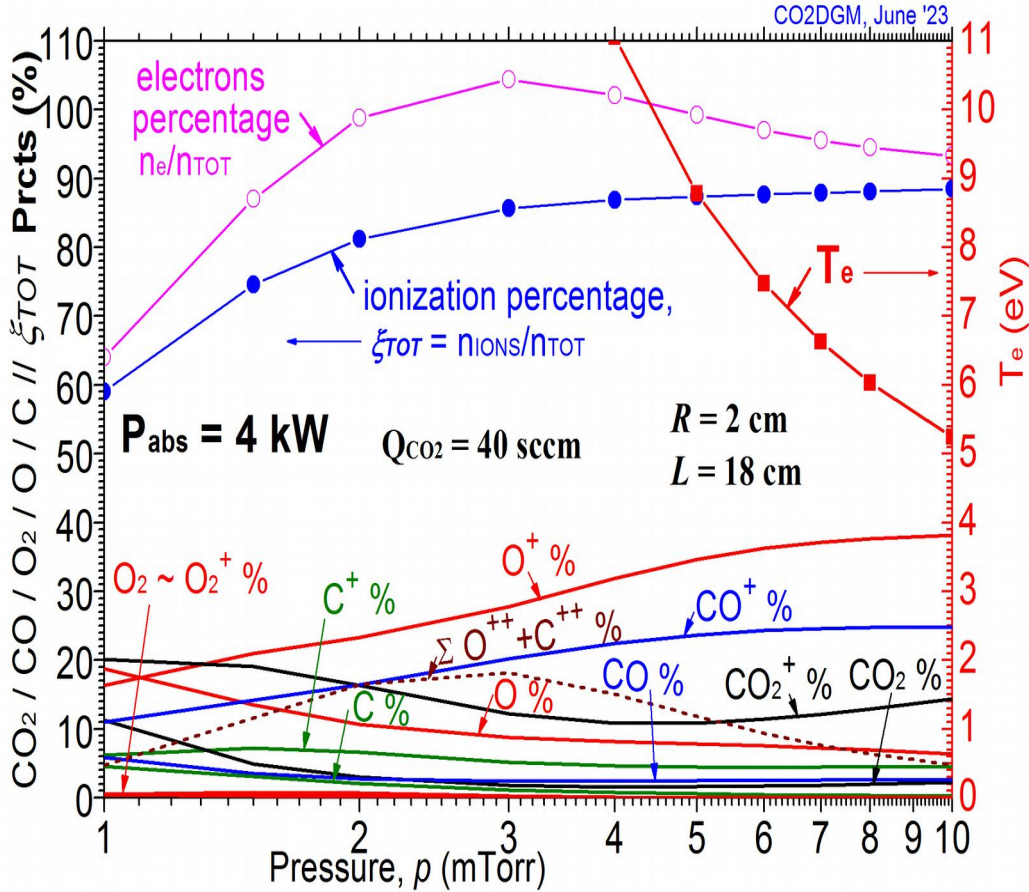


Figure 4. Pressure-dependent diagram, concomitant to the PCC of Fig. 3, $P_{abs} = 4$ kW

As was the case with Fig. 2, Fig. 4 includes the percentages of the main plasma constituents and also the total ionization percentage $\xi_{TOT} = n_{IONS} / n_{TOT}$. The electron temperature T_e values are given in the right side of the figure. Note that for the higher and the lower pressures the ξ_{TOT} values are comparable with these of the electron percentage n_e / n_{TOT} . The observed fast increase of the T_e values when pressure diminish for the lower pressure values region is very high, going mostly outside the figure.

In the lower part of Fig. 4, in accordance with results shown in Fig. 3, only presences of O^+ and CO^+ exceed practically the 20 %.

3. Functioning of ETs fueled with $Q_{TOT} = 40$ sccm of CO_2

Functioning of CO_2 -fueled ETs is investigated seeking the ionization percentages of the plasma components following isopower and isothermal curves. In so doing, the necessary FDs have been obtained on the basis of the CO2DGM results. In the present section, such a diagram is presented, corresponding to parameters and conditions pertaining to the cases addressed in the previous section. PCC and concomitant diagrams presented in Section 2, provide only two snapshots of the plasma composition of a CO_2 fed thruster under the given conditions. In fact, CO2DGM may result to a condensed description of ET functioning under various corresponding conditions. Such FD-based descriptions for CO_2 plasma, but also for other propellants addressing thrusters under various conditions, have been done previously elsewhere [9,15-19].

We present here in Fig. 5 a typical pressure depending FD, describing the functioning of a Helicon type ET with the characteristics and in conditions addressed in Section 2. Results of absorbed powers span the region from 0.5 W to 4.0 kW (blue isopower curves with stars). Corresponding electron temperatures vary from $T_e = 3.5$ eV to $T_e = 40$ eV (red isothermal curves with full circles) in case of 40 sccm CO_2 fueling. Characteristics of the two PCC diagrams already presented in Section 2 are embedded in Fig. 5. However, this figure contains additional CO2DGM results, related to

PCCs which have not been included in Section 2 for lack of space.

It is possible to observe in Fig. 5 that in the case of lower P_{abs} values the provided power is mostly spend to chemical reactions without contributing to consistent ionization percentage. It can also be seen that, once the propellant feed has been selected, the ionization level depends essentially on the total pressure and on the absorbed power.

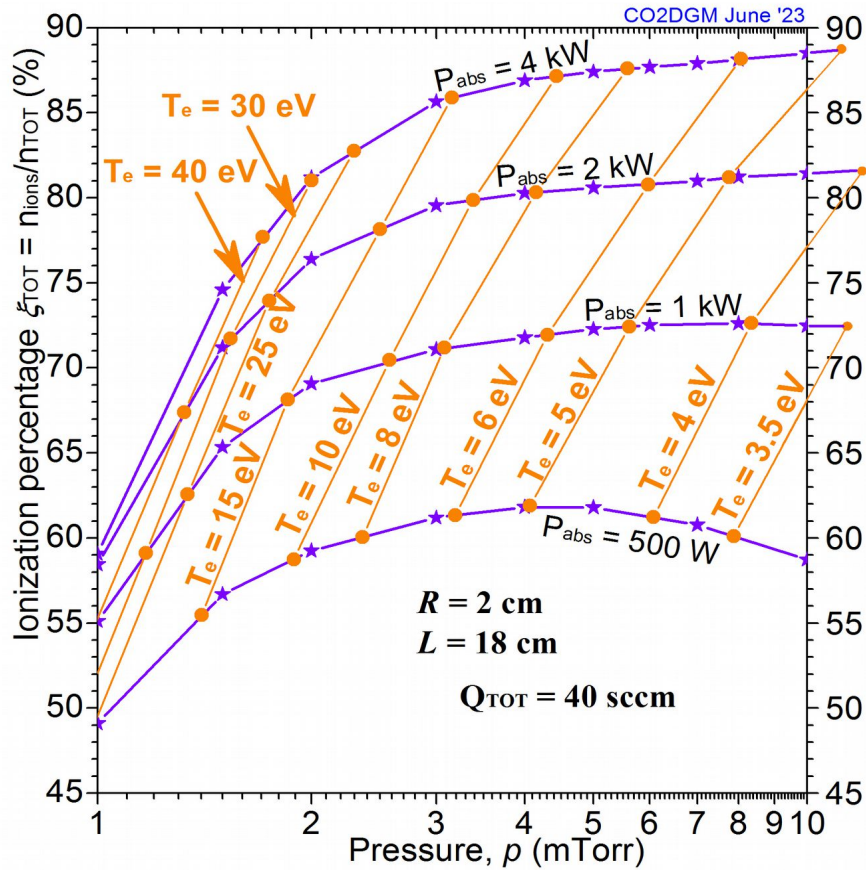


Figure 5. Pressure-dependent FD

Note that we address here an ISRU type technology, hence the availability of the propellant could become an important issue only in case of projects addressing missions in the Near Mars Trips (NMT) and Near Venus Trips (NVT), which may be away from regions insuring sufficient availability of the propellant.

4. CO₂ plasma OES diagnostics based on CO2DGM results

Optical diagnostics has been successfully used in diagnosing CO₂ plasma, as reported e.g. in [1,3,9-12,14,20]. Non-perturbing OES diagnostics is addressed here, also based on the spectra of neutral and of singly ionized oxygen and carbon species. The theoretical spectra of these species have been obtained by calculations based on the CO2DGM model, while the experimental ones must be acquired experimentally each time from the corresponding plasma to be diagnosed. It has been often verified that OES diagnostics leads to reliable results in the laboratory and in the industry notably of interest to space technology, whenever detailed experimental and theoretical spectra are available for comparison. Obviously, in order to obtain detailed theoretical spectra of the plasma, an extended set of data have been included in the model. These have been described elsewhere. However, data from [21] play an essential role. Related calculations have been also made following [22]. More generally, we have used theoretical values pertaining to the atomic components of space interest propulsion plasma either for Collisional – Radiative (C-R) modeling for argon [23-25] and for xenon [23,26,27] or with DGMs for xenon [19], for iodine [16,28,29] and for CO₂ [20].

Here, the possibility of using both oxygen and carbon species allows for an advantageous comparison of the corresponding diagnostics results. In so doing, the abundance of the species calculated simultaneously by the CO2DGM model are taken into consideration. A similar procedure, comparing OES results from hydrogen and from helium spectra of the same plasma is addressed in [30,31], see also the poster by Katsonis and Berenguer [8], this Conference.

As an example of the theoretical oxygen spectra obtained by CO2DGM we present in Figs. 6 and 7 the main lines of the neutral oxygen and carbon spectra correspondingly. The most intense theoretical lines in these figures belong to

VUV region, with their intensities divided by 100 in order to fit adequately in the figures. Handling experimentally of VUV spectra is rather cumbersome, therefore we propose to use spectra belonging to the UV and visible regions. Large spectral regions are addressed by our calculations, including the VUV, UV, visible and IR regions, for typical conditions as noted in the figures. The addressed absorbed power is of 1 kW, which corresponds to the first example of Section 2, Figs. 1, 2.

Multiplet identification and evaluated intensities are given in Figs. 6 and 7 using various colors, seeking a clear description of the spectra. The corresponding cores are also given in parenthesis and the individual line intensities are marked by short horizontal lines.

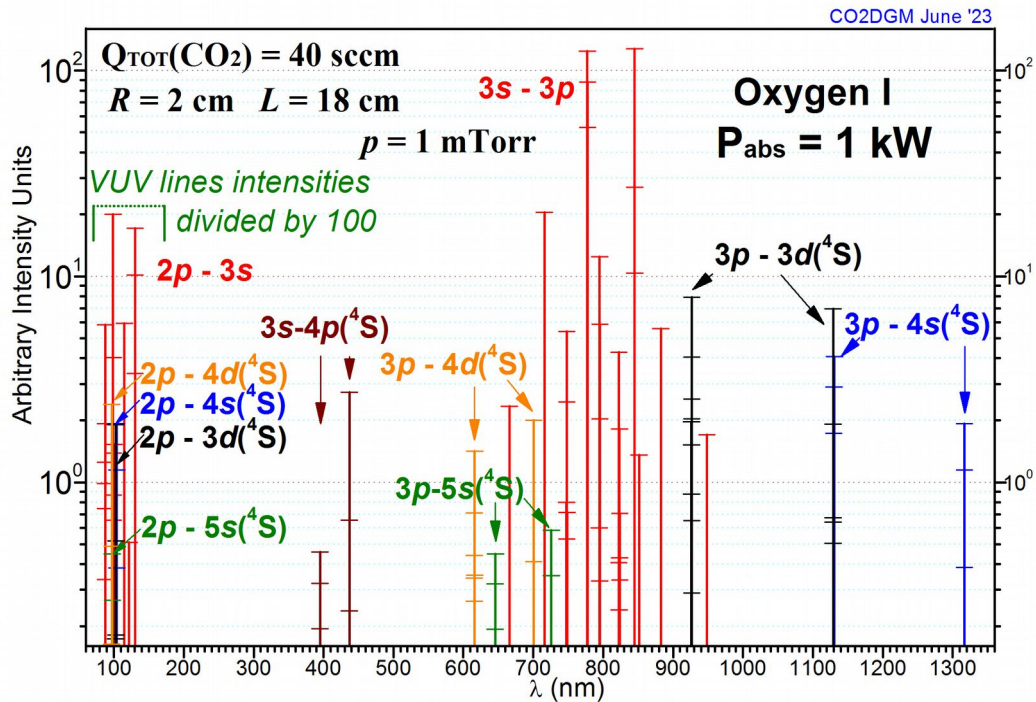


Figure 6. Extended O I theoretical spectrum from the VUV up to IR regions

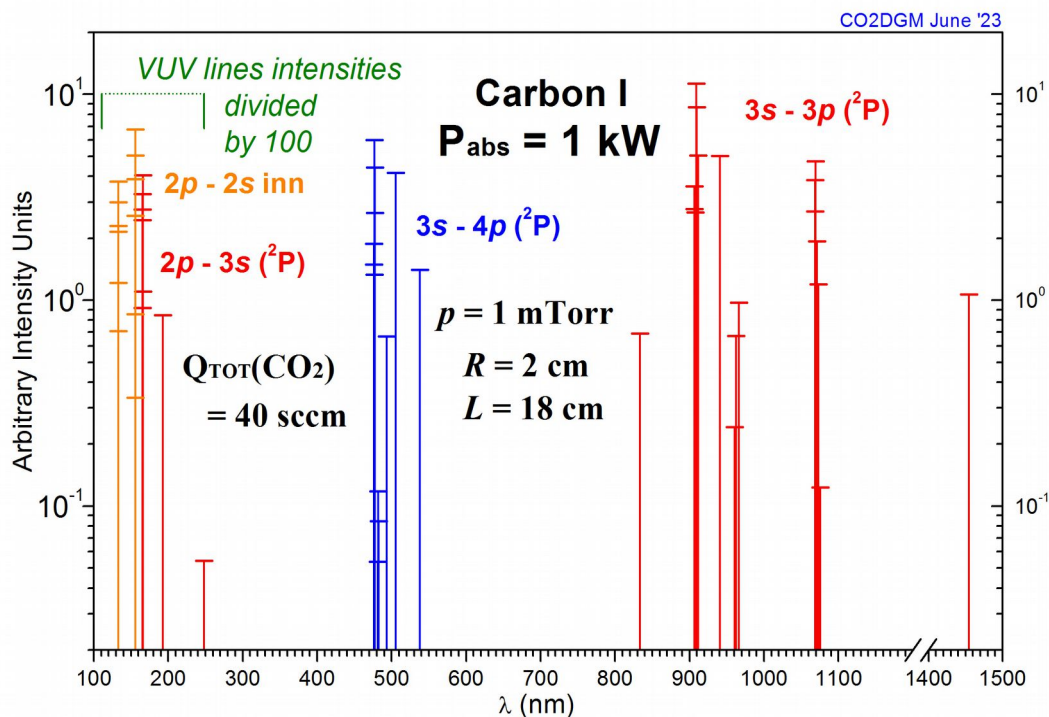


Figure 7. As in Fig. 6, but for C I spectrum

Main theoretical spectral lines of O II and C II, roughly in the 50 nm to 700 nm region, are given in Figs. 8 and 9. These ionized species spectra pertain to the same conditions with those of Figs. 6 and 7. Both are covering smaller wavelength ranges. The spectra have been calculated simultaneously with those of the neutral O and C species. Multiplets and cores are also noted occasionally in Figs. 8 and 9, as was the case with Figs. 6 and 7.

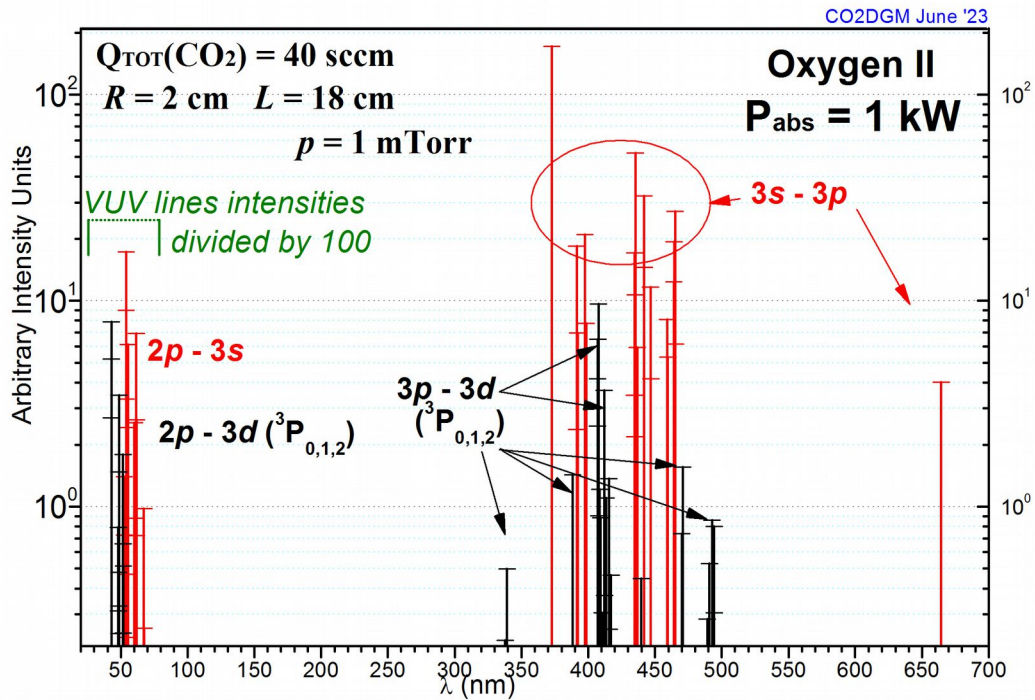


Figure 8. O II theoretical spectrum from the VUV up to optical regions

When spectra are acquired in the OES context, comparison of experimental lines obtained by spectral acquisition with the theoretical ones shown in Figs. 6, 7 and Figs. 8, 9 result straightforwardly to important plasma parameter values as electron density and temperature and ionization level. Thus, it becomes possible to obtain characterization and monitoring of the studied device on the basis of the modeling and the OES diagnostics of its plasma.

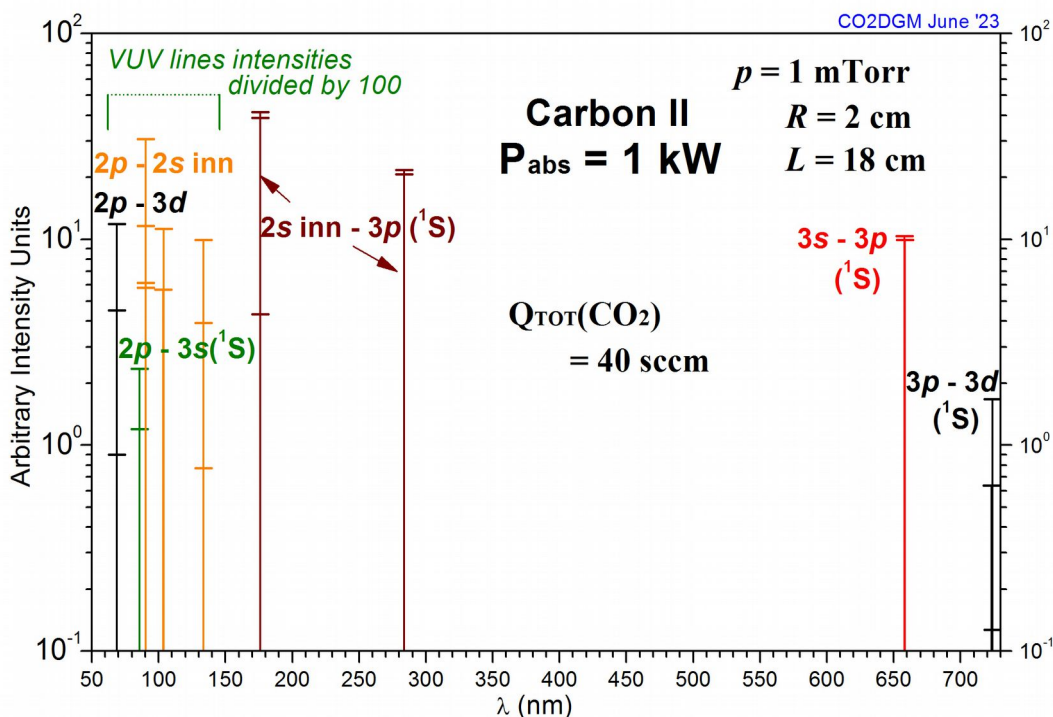


Figure 9. As in Fig. 8, but for C II spectrum

5. Conclusions and perspectives

The PCC and FD diagrams and theoretical oxygen and carbon I and II spectra obtained from CO2DGM and presented and discussed in Sections 2-4 contribute efficiently to characterize theoretically and to diagnose prototype CO₂ fed thrusters. Absorbed power values from 0.5 kW to 4 kW have been addressed here, for a total CO₂ flow rate of 40 sccm and pressures going from 1 mTorr to 10 mTorr.

CO2DGM is able to strongly support characterization and diagnostics of CO₂-fueled ETs, notably those which take advantage of ISRU technology. It will considerably contribute to the optimization of such ETs, which are expected to be applied in satellite propulsion e.g. in the MAtm and VAtm.

More generally, besides Mars and Venus satellites, NMT and NVT missions should take advantage of CO₂ propellant harvested from MAtm and VAtm.

References

- [1] Katsonis, K., Berenguer, Ch. and Cesaretti, G. (2020). *ISRU Technology Propulsion for Missions in the Solar System*, 1st Aerospace Europe Conference, AEC2020-523, Bordeaux, France, 25 to 28 February 2020
- [2] Berenguer, Ch. and Katsonis, K. (2016). *A Detailed Global Model for Characterization of CO₂ Fed Electric Thrusters*, *Imperial Journal of Interdisciplinary Research* **2**, 1708
- [3] Katsonis, K. and Berenguer, Ch. (2018). *Characterization and Optical Diagnostics of CO₂ Fed Electric Thrusters by Using a Detailed Global Model*, 6th Space Prop. Conf., Paper ID SP2018_00237, Seville, Spain, May 2018
- [4] Katsonis, K. and Berenguer, Ch. (2023). *Support of Solar system study by using ISRU based electric propulsion : The case of Neptune*, ESA Topic 14 Workshop, Innovative propulsion on Non-terrestrial bodies, June 29, 2023
- [5] Berenguer, Ch. and Katsonis, K. (2023). *Atmospheric remnants as propellant for space electric propulsion*, Electric Propulsion Innovation & Competitiveness Workshop EPIC, Naples, Italy, May 2023
- [6] Berenguer, Ch. and Katsonis, K. (2023). *Earth atmosphere remnants as an electric propulsion propellant*, Aerospace Europe Conference 2023, Lausanne, Switzerland, July 2023
- [7] Katsonis, K. and Berenguer, Ch. (2023). *Exploration of the Neptune vicinity using ISRU technology*, Electric Propulsion Innovation & Competitiveness Workshop EPIC, Naples, Italy, May 2023
- [8] Katsonis, K. and Berenguer, Ch. (2023). *ISRU electric propulsion in the Neptune vicinity*, Poster, Aerospace Europe Conference 2023, Lausanne, Switzerland, July 2023
- [9] Berenguer, Ch., Katsonis, K. and Gonzalez del Amo, J. (2020). *CO₂ Based ISRU Propulsion for Satellites and Spacecrafts in the Vicinity of Mars*, 1st Aerospace Europe Conference, AEC2020_525, Bordeaux, France, 25 February 2020
- [10] Katsonis, K. and Berenguer, Ch. (2018). *The CO2DGM for CO₂ – Breathing Thrusters*, EPIC 2018 Workshop, London, UK, October 2018
- [11] Katsonis, K., Berenguer, Ch., Gonzalez del Amo, J. and Stavrinidis, C. (2016). *CO₂ / N₂ Breathing Electric Thrusters for LMOs*, 5th Space Prop. Conf., Paper ID SP2016_3124972 Rome, Italy, May 2016
- [12] Katsonis, K. and Berenguer, Ch. (2014). *Characterization of Low Pressure CO₂ Plasmas in Space*, ESA 6th RHTG Workshop, St. Andrews, UK, November 2014
- [13] Berenguer, Ch. and Katsonis, K. (2014). *Global Modeling of CO₂ Discharges with Aerospace Applications*, *Advances in Aerospace Engineering* **2014**, Paper ID 847097
- [14] Berenguer, Ch., Katsonis, K. and Gonzalez Del Amo, J. (2021). *Spacecraft Propulsion with ISRU Near Mars and Venus, Based on CO₂ Propellant*, 7th Space Propulsion 2020+1 Conference, SP2020_016, Estoril, Portugal, March 2021
- [15] Berenguer, Ch. and Katsonis, K. (2018). *Detailed Global Modeling in Support of Electric Propulsion and Throttling of Common Propellants*, 6th Space Propulsion Conference, Paper ID SP2018_245, Seville, Spain, May 2018
- [16] Katsonis, K. and Berenguer, Ch. (2016). *A Detailed Global Model of Iodine Plasma for Optimization and Diagnostics of Electric Thrusters*, *Imperial Journal of Interdisciplinary Research* **2**, Issue 12, 166, p. 1093, November 2016
- [17] Berenguer, Ch. and Katsonis, K. (2018). *Characterization and Optical Diagnostics of Air – Breathing Electric Thrusters by 4CDGM*, EPIC 2018 Workshop, London, UK, October 2018
- [18] Katsonis, K., Berenguer, Ch. and Gonzalez del Amo, J. (2018). *An Indium Detailed Global Model for FEED Thrusters Characterization and Optical Diagnostics*, 6th Space Propulsion Conference, Paper ID SP2018_097, Seville, Spain, May 2018
- [19] Katsonis, K., Berenguer, Ch., Pavarin, D., Trezzolani, F., Manente, M. and Gonzalez del Amo, J. (2018). *A Xenon Detailed Global Model in Support of Electric Propulsion Technology*, 6th Space Propulsion Conference, Paper ID SP2018_212, Seville, Spain, May 2018

- [20] Berenguer, Ch., Katsonis, K., Herdrich, G. and Burghaus, H. (2019). *A Detailed Global Model for Modeling and Optical Diagnostics of Low Power Propulsion Devices Fed by CO₂*, IEPC-2019-**682**, 36th International Electric Propulsion Conference, Vienna, Austria, September 2019
- [21] Kramida, A., Ralchenko, Yu., Reader, J. and NIST ASD Team (2022). *NIST Atomic Spectra Database (ver. 5.10)*, <http://physics.nist.gov/asd>, Gaithersburg, MD, USA
- [22] Kramida, A. (2018). *A Suite of Atomic Structure Codes Originally Developed by RD Cowan Adapted for Windows-Based Personal Computers*, National Institute of Standards and Technology, Gaithersburg, MD, USA
- [23] Katsonis, K., Pellerin, S. and Dzierzega, K. (2003). *C-R type Modeling and Application in Plasma Diagnostics*, JHTMP **7**, 559
- [24] Katsonis K, Boisse-Laporte C, Bonnet J, Letout S. and Siskos A. (2004). *C-R Modeling and Spectroscopic Diagnostics of SPT Plasmas*, 4th International Spacecraft Propulsion Conference, 2004ESASP.555E.**129K**, Cagliari, Sardinia, Italy, 2-4 June 2004
- [25] Katsonis, K., Berenguer, Ch., Pavarin, D., Lucca Fabris, A., Trezzolani, F., Faenza, M., Tsekeris, P., Cohen, S. and Cornille, M. (2011). *Optical Diagnostics of a Low Temperature Argon Thruster*, 32nd International Electric Propulsion Conference, IEPC-2011-**169**, Wiesbaden, Germany, September 11 – 15, 2011
- [26] Katsonis, K., Cornille, M., Siskos, A. and Tanguy, M. (2004). *Low Temperature Validation of a Xe C-R Plasma Model*, 4th International Spacecraft Propulsion Conference, 2004ESASP.555E.**130K**, Cagliari, Sardinia, Italy, 2-4 June 2004
- [27] Katsonis, K., Berenguer, Ch., Clark, R.E.H., Cornille, M. and Ganciu, M. (2007). *Collisional-Radiative Models for Diagnosis of Xe Plasmas*, ECAMP IX Conference, Crete, Greece, 7-11 May 2007
- [28] Katsonis, K., Berenguer, Ch., Scharmann, S., Gärtner, W., Holste, K., Köhler, P., Mitic, S. and Klar, P.J. (2016). *Model Based Development of Electric Thrusters Using Iodine Propellant*, 5th Space Propulsion Conference, Paper ID SP2016_ **3125322**, Rome, Italy, May 2016
- [29] Berenguer, Ch., Katsonis, K. and Gonzalez del Amo, J. (2018). *Using of an Iodine Detailed Global Model for Characterization and for Optical Diagnostics of Helicon Thrusters*, 6th Space Propulsion Conference, Paper ID SP2018_ **215**, Seville, Spain, May 2018
- [30] Katsonis, K., Berenguer, Ch., Walpot, L. and Gonzalez Del Amo, J. (2021). *A Detailed Global Model of Hydrogen / Helium in Support of Neptune Study*, 7th Space Propulsion 2020+1 Conference, SP2020_ **384**, Estoril, Portugal, March 2021
- [31] Berenguer, Ch., Katsonis, K. and Gonzalez del Amo, J. (2022). *Using the Constituents of the Giant Planets Atmospheres as ISRU Propellants for Electric Thrusters*, SP2022_ **079**, 8th Space Propulsion Conference, Estoril, Portugal, May 2022